

# CHORUS

This is the accepted manuscript made available via CHORUS. The article has been published as:

## Role of Lattice Coupling in Establishing Electronic and Magnetic Properties in Quasi-One-Dimensional Cuprates

W. S. Lee, S. Johnston, B. Moritz, J. Lee, M. Yi, K. J. Zhou, T. Schmitt, L. Patthey, V. Strocov, K. Kudo, Y. Koike, J. van den Brink, T. P. Devereaux, and Z. X. Shen

Phys. Rev. Lett. **110**, 265502 — Published 25 June 2013

DOI: [10.1103/PhysRevLett.110.265502](https://doi.org/10.1103/PhysRevLett.110.265502)

# The Role of Lattice Coupling in Establishing Electronic and Magnetic Properties in Quasi-One-Dimensional Cuprates

W. S. Lee,<sup>1,\*</sup> S. Johnston,<sup>1,2</sup> B. Moritz,<sup>1,3,4</sup> J. Lee,<sup>5</sup> M. Yi,<sup>5</sup> K. J. Zhou,<sup>6</sup> T. Schmitt,<sup>6</sup> L. Patthey,<sup>6</sup> V. Strocov,<sup>6</sup> K. Kudo,<sup>7</sup> Y. Koike,<sup>7</sup> J. van den Brink,<sup>2</sup> T. P. Devereaux,<sup>1</sup> and Z. X. Shen<sup>1</sup>

<sup>1</sup>*SIMES, SLAC National Accelerator Laboratory, Menlo Park, CA 94025, USA*

<sup>2</sup>*IFW Dresden P.O. Box 27 01 16, D-01171 Dresden, Germany*

<sup>3</sup>*Department of Physics and Astrophysics, University of North Dakota, Grand Forks, ND 58202, USA*

<sup>4</sup>*Department of Physics, Northern Illinois University, DeKalb, IL 60115, USA*

<sup>5</sup>*Department of Applied Physics, Stanford University, Stanford, CA 94305, USA*

<sup>6</sup>*Paul Scherrer Institut, Swiss Light Source, CH-5232 Villigen PSI, Switzerland*

<sup>7</sup>*Department of Applied Physics, Tohoku University, Japan*

(Dated: April 26, 2013)

High resolution resonant inelastic x-ray scattering has been performed to reveal the role of lattice-coupling in a family of quasi-1D insulating cuprates,  $\text{Ca}_{2+5x}\text{Y}_{2-5x}\text{Cu}_5\text{O}_{10}$ . Site-dependent low energy excitations arising from progressive emissions of a 70 meV lattice vibrational mode are resolved for the first time, providing a direct measurement of electron-lattice coupling strength. We show that such electron-lattice coupling causes doping-dependent distortions of the Cu-O-Cu bond angle, which sets the intra-chain spin exchange interactions. Our results indicate that the lattice degrees of freedom are fully integrated into the electronic behavior in low dimensional systems.

PACS numbers: Valid PACS appear here

Electron-lattice coupling is an important mechanism in solids that determines the ground state properties via renormalizing the mass of charge carriers [1], and, in some cases, induces novel symmetry-broken states like superconductivity [2] and charge density waves [3]. While research on the electron-lattice interaction has a long history in condensed matter physics, it continues to be an important topic in establishing new paradigms for understanding the properties of strongly correlated materials in which charges become more localized and screening effects are weak [4]. To date the electron-lattice coupling in two dimensional correlated materials such as cuprates [5–9] and manganites [10–12] has drawn much attention in the field. In one dimensional (1D) cuprate systems, although unusual spin and charge dynamics [13–17] have been revealed, studies of the role of electron-phonon coupling are still lacking. Such studies are important since poor screening effects in 1D systems [18] should in principle cause strong electronic coupling to the lattice.

To address this issue, we study a family of quasi-1D cuprates  $\text{Ca}_{2+5x}\text{Y}_{2-5x}\text{Cu}_5\text{O}_{10}$ , in which  $\text{CuO}_2$  plaquettes arrange in a chain-like structure by sharing their edges with neighboring  $\text{CuO}_2$  plaquettes. This system is important as it is the only quasi-1D cuprate that can be doped over a wide range of hole concentrations, providing a unique opportunity to study doping induced phenomena [19, 20]. By increasing carrier concentration, the spin ground state evolves from A-type antiferromagnetic order (intra-chain ferromagnetic order with inter-chain antiferromagnetic alignment), to spin glass, followed by spin gap, and eventually to a spin disordered phase [20, 21]. Curiously, the structural Cu-O-Cu bond angle, which determines to the size and sign of the spin

super-exchange interaction according to Goodenough-Kanamori-Anderson theory [13, 22–24], is also doping dependent [20]. However, the important mechanism behind the doping induced Cu-O-Cu angle change remains unclear. Using high resolution resonant inelastic x-ray scattering (RIXS), we find a 70 meV phonon strongly coupled to the electronic state. As we will demonstrate, the doping dependent Cu-O-Cu angle is driven by electron-lattice coupling due to the ineffectiveness of screening in 1D. Further, the phonon energy is found to soften when cooling across the antiferromagnetic phase transition in the undoped compounds. These observations demonstrate that the lattice degrees of freedom are fully integrated into the electronic and magnetic properties of low-dimensional correlated materials.

Single crystals of  $\text{Ca}_{2+5x}\text{Y}_{2-5x}\text{Cu}_5\text{O}_{10}$  used in the present study were grown by traveling-solvent floating-zone (TSFZ) methods. Samples with three different doping levels were selected for measurements, nominally  $x = 0, 0.3, \text{ and } 0.33$ . The RIXS measurements were performed at the ADDRESS beamline, Swiss Light Source, with the energy resolution set at either 50 meV or 80 meV. The sample surface was the (0, 1, 0) plane, coincident with the chain plane, prepared by either polishing ( $x = 0$ ) or cleaving ( $x = 0.3 \text{ and } 0.33$ ). The scattering angle was set at 90 degree to minimize the elastic peak intensity. As sketched in Fig. S1(c) in the Supplementary Material, the scattering plane was the a-b plane with a grazing angle of 20 degree to the sample surface. The polarization of the incident photon is perpendicular to the scattering plane ( $\sigma$ -polarization), while the recorded spectrum includes all the polarizations of the scattered photons.

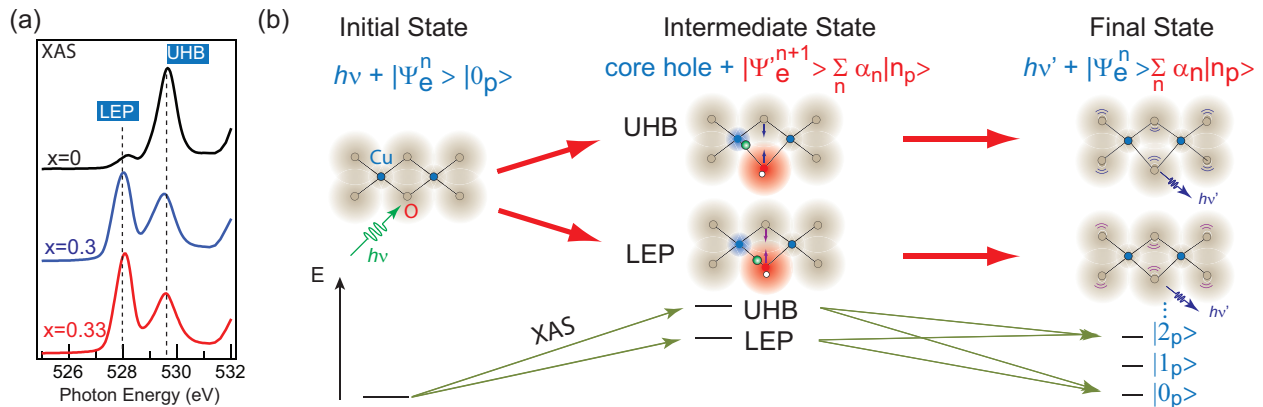


FIG. 1: (color online) (a) x-ray absorption spectrum near the oxygen  $K$ -edge for  $\text{Ca}_{2+5x}\text{Y}_{2-5x}\text{Cu}_5\text{O}_{10}$  compounds of three different doping levels. The “UHB” and “LEP” denotes the absorption peaks at 529.5 and 528 eV, respectively. The average number of hole per Cu ion is denoted as  $x$ . (b)  $|\Psi_e^n\rangle$  and  $|\Psi_e^{n+1}\rangle$  denotes the electronic ground state and the excited electronic intermediate state with an additional electron excited from the oxygen  $1s$  core level.  $|n_p\rangle$  ( $n = 0, 1, 2, \dots$ ) denotes the number of phonon quanta excited in the lattice degree of freedom with a wavefunction superposition coefficient  $\alpha$ . For purposes of illustration, the wavefunction is expressed as product states of the diagonalized electron and lattice Hamiltonians. Here, the lattice vacuum state  $|0_p\rangle$  is referenced to the initial equilibrium phonon occupation and  $|n_p\rangle$  describes excitations from this state. In the RIXS intermediate state, an electron (green ball) is excited, leaving a core hole (white ball) in the O  $1s$  level. The excited electron can be closer to either Cu or O site by tuning the incident photon energy to match the UHB or LEP resonance, respectively. The change of the local charge density on Cu (blue shade) and O (red shade) sites induce local relaxation of the distorted lattice, creating a distribution of  $|n_p\rangle$ . In the final state, the excited electron can recombine with the core hole, leaving the lattice in excited states. These final states have non-zero overlap with the intermediate state, yielding harmonic phonon excitations in RIXS spectrum.

It is informative to first introduce the doping evolution of the electronic wave function, revealed by the x-ray absorption spectrum (XAS) near the O  $K$ -edge ( $1s$ - $2p$  transition). As shown in Fig. 1(a), the XAS of the undoped compound exhibits a single dominant absorption peak (529.5 eV), which is associated with the upper Hubbard band (UHB). Upon hole-doping, the UHB peak decreases, indicating a reduction of the weight of the UHB component [25]. In addition, a lower energy peak (LEP) emerges, which arises from the spectral weight transfer to wavefunction components that are directly related to the doped holes [26]. Approximately, in real space, the XAS at the UHB resonance produces a final state with one additional valence electron near the copper site, while the XAS at the LEP resonance puts the additional valence electron near the oxygen site, as sketched in Fig. 1(b). We note that although our undoped sample is nominally  $x = 0$ , the presence of small weight of LEP indicates that our “undoped” compound might be slightly self-doped via impurities. Judging from the LEP spectral weight, the effective doping is estimated to be at most  $x = 0.017$ . The presence of such a small concentration of dopants in our undoped sample does not change our discussions presented in this letter.

To investigate the effects of lattice coupling on the electronic states, we use resonant inelastic x-ray scattering (RIXS) [27, 28]. The underlying principle is illustrated in Fig. 1(b). In the O  $K$ -edge RIXS process, a  $1s$  core electron will first be excited into an XAS final state, either

the UHB or LEP resonance. This causes a local change in the charge density which locally distorts the lattice. Later, the electron de-excites, filling the O  $1s$  core hole, leaving the lattice in an excited state. The RIXS spectrum records the overlaps of the initial, intermediate, and final states as a function of energy loss (the energy difference between the incident and emitted photons), and includes the possibility of producing multiple peaks in the spectrum with an energy separation corresponding to the energy of the quanta of the lattice vibrations (i.e. phonons) in a fashion analogous to a generalized Frank Condon picture. The spectral weight of phonon excitations in the RIXS spectrum is directly dependent on the electron-phonon (e-ph) coupling strength. Furthermore, the e-ph coupling strength at Cu and O sites can be determined by tuning the incident photon energy to the UHB and LEP resonances, respectively. This site dependency stems from differences in the electronic character of the XAS final states.

Figure 2(a) displays RIXS spectra for the undoped parent compound. As the incident photon energy is tuned to near the UHB resonance (‘e’ and ‘f’), the spectra near the elastic scattering peak, develops an unusual asymmetric broadening, indicating the excitations of low energy modes. Upon doping, as shown in Fig. 2(b), an asymmetric spectrum near the elastic peak is also observed at the UHB resonance, however it is now most pronounced at the LEP resonance. The shift of resonance behavior is associated with the doping evolution of the XAS spec-

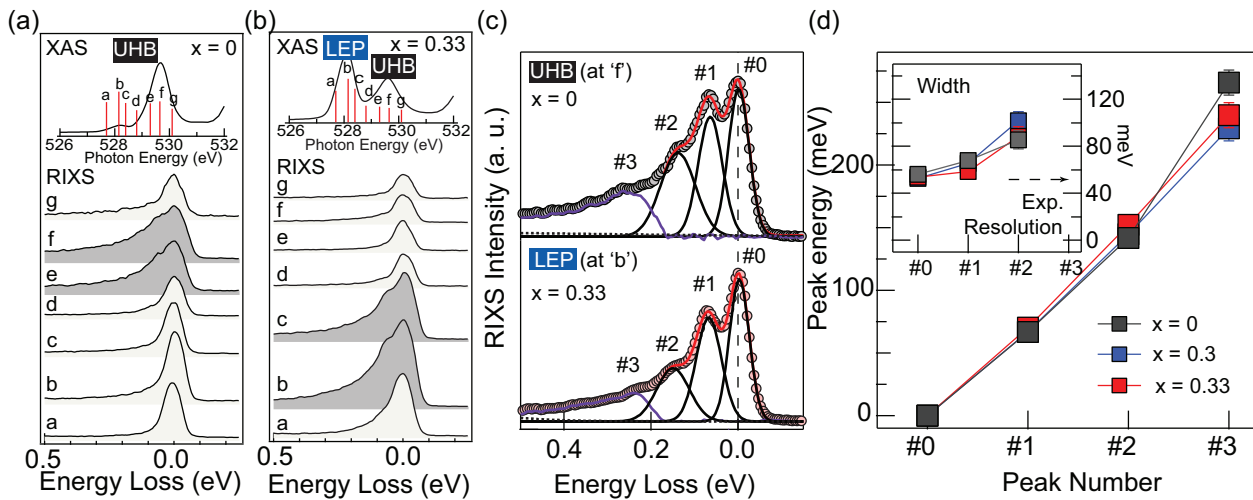


FIG. 2: (color online) The RIXS spectrum for (a)  $x = 0$  and (b)  $x = 0.33$  samples taken at several incident photon energies, as indicated by the red bars in the XAS plots. The length of these red vertical bars reflects the relative elastic peak intensity of the corresponding RIXS spectrum. The darker shaded areas highlight the spectra with prominent additional spectral weight near the elastic peak. (c) High resolution data taken at UHB resonance for the  $x = 0$  sample (upper) and at LEP resonance for the  $x = 0.33$  sample (lower). Multi-peak features are annotated with number identifiers. The black curves are the Gaussian functions used for the fit (red curves). Purple curves are the remaining spectrum after subtracting the fit. Background is plotted as black dotted lines. (d) A summary plot of the fitted peak positions and widths (inset) of the RIXS spectra taken at UHB ( $x = 0$ ) and LEP ( $x = 0.3$  and  $0.33$ ) resonances. All data were taken at 30 K.

tral weight due to changes of the wavefunction character [26], suggesting that the origin of the low-energy modes is coupled directly with the electronic wavefunction.

Higher resolution RIXS spectra (Fig. 2(c)) provide further information about the origin of these low-energy excitations. At both UHB and LEP resonances, we resolved multiple peaks in the spectrum, which lie in harmonic order of a single energy scale of 70 meV (Fig. 2d). We note that since the spin super-exchange energy (10-14 meV) [25, 29] is much smaller than the extracted mode energy, the observed excitations cannot be attributed to spin excitations. Rather they are most likely due to an oxygen bond-stretching vibrational mode, similar to those commonly found in 2D cuprates at a similar energy scale [5]. In addition, the mode energy extracted from the RIXS spectra taken at the UHB and LEP are identical, indicating that the observed phonon excitations share the same origin. These observations demonstrate that the electronic states in the CYCO system are coupled strongly with this 70 meV phonon mode.

To gain further insight into harmonic progression of phonon excitations, we use exact diagonalization to calculate RIXS for  $\text{CuO}_2$  clusters coupled to a subset of optical oxygen vibrations. In this model, we include coupling to a vibrational mode whose eigenvector is sketched in Fig. 3(a) with coupling strengths of  $g_{Cu}$  and  $g_O$  on Cu and O sites, respectively. (Supplementary Material) This mode derives its coupling from the strong electrostatic modification it produces to the electronic states of the edge-shared  $\text{CuO}_2$  chains (Supplementary Mate-

rial). Our calculations (Fig. 3(a)) capture the essential physics related to the observed excitations, reproducing the XAS spectrum, the phonon excitations, and their shift from the UHB to LEP resonance in the doped cluster. Importantly, we show that their spectral weight is extremely sensitive to the e-ph coupling strength: the stronger the coupling, the greater the spectral weight for higher-harmonic phonon excitations (Fig. 3(b)). In addition, our calculation explicitly demonstrates that the difference between  $g_{Cu}$  and  $g_O$  can be resolved by comparing the RIXS spectrum taken at the UHB and LEP resonances (Fig. 3(c)). This site dependent information is unique to RIXS and confirms the concepts illustrated in Fig. 1b. We note that our calculations cannot reproduce the broadening of the higher harmonic phonon emission as plotted in the inset of Fig. 2(d), which we believe is caused by a small dispersion of the phonon branch. Due to the exponential growth of the Hilbert space, treating such a dispersive phonon is beyond our capabilities.

With these insights, we can compare the electron-lattice coupling strength via the spectral shape of the phonon excitations. First, as shown in Fig. 3(d), we found that the coupling strength is essentially doping independent, even though a significant number of holes are doped into the system. This demonstrates that screening remains ineffective upon doping, as expected for a one dimensional system [18]. Second, the coupling at the UHB resonance is found to be stronger than at the LEP resonance, which is caused by the difference between  $g_{Cu}$  and  $g_O$ . Within our model, the electron-phonon

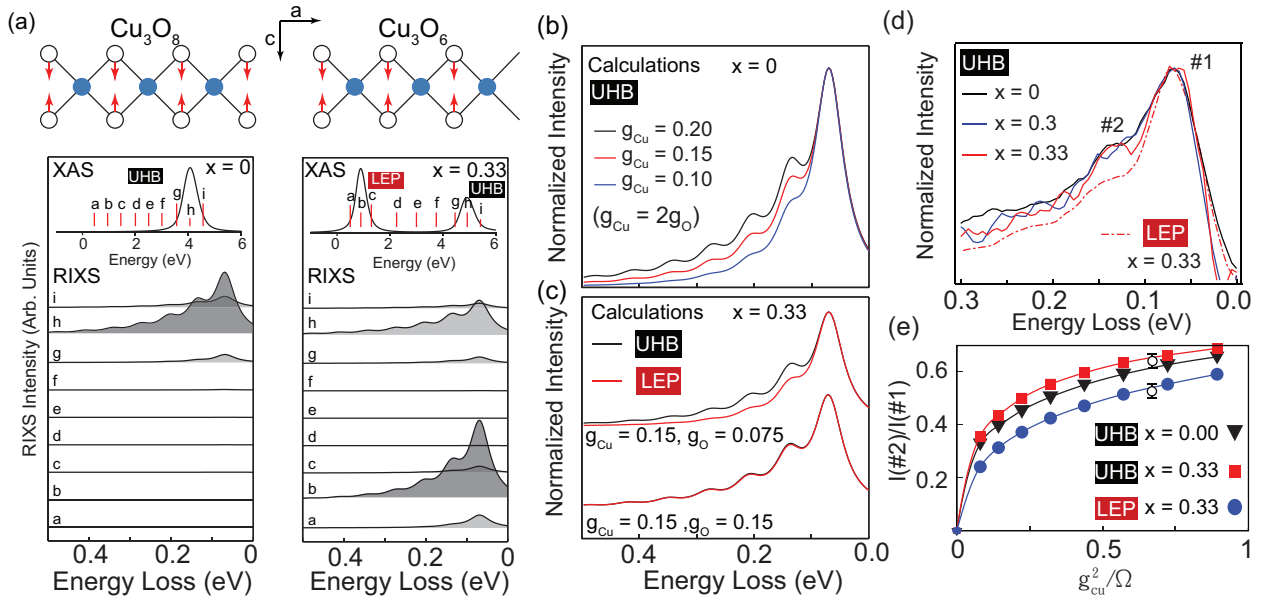


FIG. 3: (color online) (a) The calculated RIXS intensities for the  $x = 0$  (left) and  $x = 0.33$  (right) hole-doped systems, respectively, with  $g = 0.2$  eV. The incident photon energies are indicated in the calculated XAS spectra and the elastic line has been removed by excluding the ground state from the final state summation. The calculations were performed on  $\text{Cu}_3\text{O}_8$  and  $\text{Cu}_3\text{O}_6$  clusters (open and periodic boundary conditions) for the  $x = 0$  and  $x = 0.33$  cases, respectively. The arrows indicate the displacement pattern of the phonon eigenvector involving  $c$ -axis motion of the O atoms. (b) A comparison of the normalized phonon excitations at the UHB resonance for the  $x = 0$  case and different coupling strengths. (c) The normalized phonon excitation spectrum at the LEP and UHB resonance in a doped cluster ( $x = 0.33$ ). Spectra of two different values of  $g_{\text{O}}$  were calculated to demonstrate the site dependence of the RIXS process at the LEP and UHB resonances. (d) Experimental data of harmonic phonon excitations (elastic peak and background subtracted) normalized to the first phonon peak intensity at the UHB resonance for three different doping levels. Data of  $x = 0.33$  sample taken at LEP resonance is also superimposed, illustrating the site-dependent electron-phonon coupling. (e) The ratio of the model RIXS intensity  $I(\#2)/I(\#1)$  at the first and second phonon as a function of dimensionless coupling constant  $g_{\text{Cu}}/\Omega$ , where  $\Omega$  is the phonon energy, 70 meV. The data points with error bars indicate the experimental value of this ratio.

coupling strength can be obtained by comparing the intensity ratio of the second and first phonon excitations observed in our data (data points in Fig. 3(e)). We find  $g_{\text{Cu}} \sim 2g_{\text{O}} \sim 0.22$  eV (or in the dimensionless unit  $g^2/\Omega \sim 0.69$ ), in agreement with our Madelung potential analysis (Supplementary Material).

A doping-independent electron-lattice coupling has an intriguing consequence to the doping evolution of the intertwined electron-lattice ground state. As shown in Fig. 4(a), the number of phonons intertwined in the ground state is larger in the doped system than in the undoped system due to the increased carrier concentration. This implies a larger lattice distortion along the  $c$ -axis and results in a larger Cu-O-Cu angle in the doped system. Within our model, we estimate a 0.16 Å contraction of O-O distance along  $c$ -axis, corresponding to a 3.7% increase of the Cu-O-Cu bond angle in the  $x = 0.33$  doped cluster. The estimation is comparable to the reported doping induced increase of the Cu-O-Cu angle ( $\sim 2.5\%$ ) [20]. Since the size and sign of the spin super-exchange coupling is sensitive to the Cu-O-Cu bond angle, this result shows that e-ph coupling strength is an important underlying mechanism to drive the lattice structure that

hosts the spin dynamics of this 1D system.

Finally, as shown in Fig. 4(b), the phonon excitations exhibit a softening of up to  $\sim 10$  meV when the system is cooled across the antiferromagnetic transition temperature  $T_N$  (30 K). Importantly, inelastic neutron scattering measurements also have reported a spin excitation hardening of approximately 1-2 meV when cooling to low temperatures [21], demonstrating a cooperative interplay between the spin, charge and lattice sectors. We also note that the coupling to the lattice is likely responsible for the unusual spectral broadening for the spin and charge dynamics in quasi-1D cuprates observed by angle-resolved photoemission spectroscopy [16], inelastic neutron scattering [25], and RIXS measurements [17, 30]. Our results emphasize that lattice coupling in low dimensional materials needs to be considered together with the spin and charge dynamics in order to obtain a holistic picture of the underlying physics.

The authors thank J. Málek, S.-L. Drechsler, and M. Berciu for useful discussions. This work was supported by the U. S. Department of Energy, Office of Basic Energy Science, Division of Materials Science and Engineering under the contract no. DE-AC02-76SF00515. S.

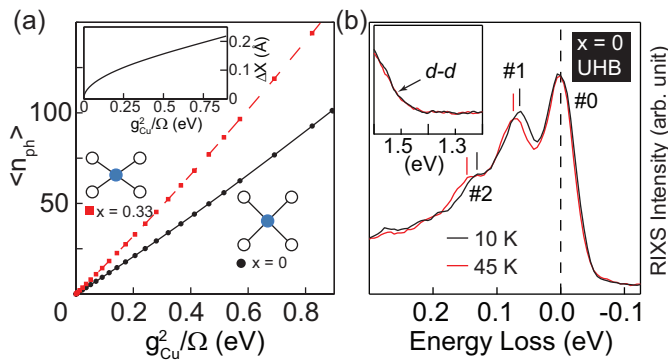


FIG. 4: (color online) (a) Calculated number of phonons entangled with the ground state wavefunction as a function of coupling strength for undoped and doped clusters. A larger number of phonon quanta in the ground state correspond to a larger lattice distortion. Please note that RIXS process excites additional phonons, leaving the system in an excited lattice state. The inset shows the estimated doping-induced changes in the lattice constant as a function of the mode coupling strength. (b) RIXS spectra taken at two temperatures across the AFM phase transition for the  $x = 0$  compound. The inset shows the rising edge of the d-d excitations. The agreement of the elastic peak and the d-d edge provide an internal energy reference, confirming the shift of the phonon mode energy across the AFM transition.

J. acknowledges funding from FOM (The Netherlands). This work was performed at the ADDRESS beamline of the Swiss Light Source using the SAXES instrument jointly built by Paul Scherrer Institut, Switzerland and Politecnico di Milano, Italy.

\* Electronic address: leews@stanford.edu

- [1] N. W. Ashcroft and N. D. Mermin, *Solid State Physics* (Saunders College Publishing, 1976).
- [2] M. Tinkham, *Introduction to superconductivity* (McGraw-Hill Book CO., 1996).
- [3] G. Gruner, *Density Waves in Solids* (ABP Perseus Publishing, 1994).
- [4] T. P. Devereaux and D. Belitz, *Phys. Rev. B* **43**, 3736 (1991).
- [5] A. Lanzara *et al.*, *Nature* **412**, 510 (2001).
- [6] K. M. Shen, F. Ronning, D. H. Lu, W. S. Lee, N. J. C. Ingle, W. Meevasana, F. Baumberger, A. Damascelli, N. P. Armitage, L. L. Miller, Y. Kohsaka, M. Azuma, M. Takano, H. Takagi, and Z.-X. Shen, *Phys. Rev. Lett.* **93**, 267002 (2004).
- [7] W. S. Lee, S. Johnston, T. P. Devereaux, and Z. X. Shen, *Phys. Rev. B* **75**, 195116 (2007).
- [8] W. Meevasana, N. J. C. Ingle, D. H. Lu, J. R. Shi, F. Baumberger, K. M. Shen, W. S. Lee, T. Cuk, H. Eisaki, T. P. Devereaux, N. Nagaosa, J. Zaanen, and Z.-X. Shen, *Phys. Rev. Lett.* **96**, 157003 (2006).
- [9] S. Johnston, I. M. Vishik, W. S. Lee, F. Schmitt, S. Uchida, K. Fujita, S. Ishida, N. Nagaosa, Z. X. Shen, and T. P. Devereaux, *Phys. Rev. Lett.* **108**, 166404 (2012).
- [10] N. Mannella, W. L. Yang, X. J. Zhou, H. Zheng, J. F. Mitchell, J. Zaanen, T. P. Devereaux, N. Nagaosa, Z. Hussain and Z.-X. Shen, *Nature* **438**, 474 (2005).
- [11] L. Vasiliu-Doloc, S. Rosenkranz, R. Osborn, S. K. Sinha, J. W. Lynn, J. Mesot, O. H. Seeck, G. Preosti, A. J. Fedro, and J. F. Mitchell, *Phys. Rev. Lett.* **83**, 4393 (1999).
- [12] A. J. Millis, P. B. Littlewood, and B. I. Shraiman, *Phys. Rev. Lett.* **74**, 5144 (1995).
- [13] Y. Mizuno, T. Tohyama, S. Maekawa, T. Osafune, N. Motoyama, H. Eisaki and S. Uchida, *Phys. Rev. B* **57**, 5326 (1998).
- [14] J. Voit, *Rep. Prog. Phys.* **58**, 977 (1995).
- [15] E. H. Lieb and F. Y. Wu, *Phys. Rev. Lett* **20**, 1445 (1968).
- [16] B. J. Kim, H. Koh, E. Rotenberg, S.-J. Oh, H. Eisaki, N. Motoyama, S. Uchida, T. Tohyama, S. Maekawa, Z.-X. Shen, and C. Kim, *Nature Phys.* **2**, 397 (2006).
- [17] J. Schlappa, K. Wohlfeld, K. J. Zhou, M. Mourigal, M. W. Haverkort, V. N. Strocov, L. Hozoi, C. Monney, S. Nishimoto, S. Singh, A. Revcolevschi, J.-S. Caux, L. Patthey, H. M. Rønnow, J. van den Brink, and T. Schmitt, *Nature* **485**, 82 (2012).
- [18] J. van den Brink and G. A. Sawatzky, *Europhys. Lett.* **50**, 447-453(2000).
- [19] A. Hayashi, B. Batlogg, and R. J. Cava, *Phys. Rev. B* **58**, 2678(1998).
- [20] K. Kudo, S. Kurogi, Y. Koike, T. Nishizaki, and N. Kobayashi, *Phys. Rev. B* **71**, 104413 (2005).
- [21] M. Matsuda, K. Kakurai, S. Kurogi, K. Kudo, Y. Koike, H. Yamaguchi, T. Ito, and K. Oka, *Phys. Rev. B* **71**, 104414 (2005).
- [22] J. B. Goodenough, *Phys. Rev.* **100**, 564 (1955).
- [23] J. Kanamori, *J. Phys. Chem. Solids* **10**, 87 (1959).
- [24] P. W. Anderson, *Solid State Phys.* **14**, 99 (1963).
- [25] M. Matsuda, H. Yamaguchi, T. Ito, C. H. Lee, K. Oka, Y. Mizuno, T. Tohyama, S. Maekawa, and K. Kakurai, *Phys. Rev. B* **63**, 180403(2001).
- [26] K. Okada and A. Kotani, *J. Phys. Soc. Japn.* **72**, 797 (2003).
- [27] L. J. P. Ament, M. van Veenendaal, T. P. Devereaux, J. P. Hill, and J. van den Brink, *Rev. Mod. Phys.* **83**, 705 (2011).
- [28] L. J. P. Ament, M. van Veenendaal, and J. van den Brink, *Europhys. Lett.* **95**, 27008 (2011).
- [29] R. O. Kuzian, S. Nishimoto, S.-L. Drechsler, J. Málek, S. Johnston, Jeroen van den Brink, M. Schmitt, H. Rosner, M. Matsuda, K. Oka, H. Yamaguchi, and T. Ito, *Phys. Rev. Lett.* **109**, 117207 (2012).
- [30] J. Schlappa, T. Schmitt, F. Vernay, V. N. Strocov, V. Ilakovac, B. Thielemann, H. M. Rønnow, S. Vanishri, A. Piazzalunga, X. Wang, L. Braicovich, G. Ghiringhelli, C. Marin, J. Mesot, B. Delley, and L. Patthey, *Phys. Rev. Lett.* **103**, 047401(2009).